HHS Public Access

Author manuscript

Mol Neurobiol. Author manuscript; available in PMC 2018 March 07.

Published in final edited form as:

Mol Neurobiol. 2018 March ; 55(3): 1977–1987. doi:10.1007/s12035-017-0467-9.

NLRP3 inflammasome inhibitor ameliorates amyloid pathology in a mouse model of Alzheimer's disease

Jun Yin[1,2], **Fanpeng Zhao**[2], **Jeremy E. Chojnacki**[3], **Jacob Fulp**[3], **William L. Klein**[4], **Shijun Zhang**[3,*], and **Xiongwei Zhu**[2,*]

[1]Department of Pathophysiology, School of Basic Medical Sciences, Wuhan University, Wuhan, Hubei, China

[2]Department of Pathology, Case Western Reserve University, Cleveland, Ohio, USA

[3]Department of Medicinal Chemistry, Virginia Commonwealth University, Richmond, Virginia 23298, USA

[4]Department of Neurobiology, Northwestern University, Evanston, Illinois, USA

Abstract

The activation of the NLRP3 inflammasome signaling pathway plays an important role in the neuroinflammation in Alzheimer's disease (AD). In this study, we investigated the effects of JC-124, a rationally designed NLRP3 inflammasome inhibitor, on AD-related deficits in CRND8 APP transgenic mice (TgCRND8). We first demonstrated increased formation and activation of NLRP3 inflammasome in TgCRND8 mice compared to non-transgenic littermate controls, which was inhibited by the treatment with JC-124. Importantly, JC-124 treatment led to decreased levels of Aβ deposition and decreased levels of soluble and insoluble $A\beta_{1-42}$ in the brain of CRND8 mice which was accompanied by reduced β-cleavage of APP, reduced activation of microglia but enhanced astrocytosis. Oxidative stress was decreased and synaptophysin was increased in the CRND8 mice after JC-124 treatment, demonstrating a neuroprotective effect. Overall, these data demonstrated beneficial effects of JC-124 as a specific NLRP3 inflammasome inhibitor in AD mouse model and supported the further development of NLRP3 inflammasome inhibitors as a viable option for AD therapeutics.

Keywords

Alzheimer's disease; amyloid-beta; inflammasome; neuroinflammation; NLRP3

INTRODUCTION

Alzheimer's disease (AD) is the most common type of dementia. Extracellular senile plaques composed of amyloid-β (Aβ) and intracellular neurofibrillary tangles composed of hyperphosphorylated tau protein, along with selective neuronal loss, are the

Correspondence and requests for materials should be addressed to X. Z. (Tel: 216-368-5903; xiongwei.zhu@case.edu); S. Z. (Tel: 804-628-8266; szhang2@vcu.edu).

Conflict of Interest Statement. None declared.

neuropathological hallmarks of AD [1]. However, the mechanisms that lead to neuronal loss and pathogenesis of AD are not completely understood [2]. Among multiple pathogenic factors implicated, neuroinflammation is believed to play a critical role in the course of the disease: Levels of inflammatory mediators, such as C-reactive protein, complement factors, chemokines and inflammatory cytokines, are elevated long before the clinical symptoms of AD [3,4]. There is strong correlation between systemic infection and the incidence of dementia [5]. Evidence suggests prolonged use of nonsteroidal anti-inflammatory drugs can prevent or delay the onset of AD [6,7]. Aβ deposition and chronic inflammatory responses interplay with each other to form a vicious cycle that expands the damaging effects [8,9]. The identification of rare mutations in TREM2 gene, encoding TREM2 protein involved in innate immune response, that increase susceptibility to late-onset AD lends strong support for a causal role of neuroinflammation in the pathogenesis of AD [10,11].

A key event in the inflammatory pathway is the activation of inflammasomes, multiprotein complexes that typically consist of a cytoplasmic sensor/receptor, an adaptor protein apoptosis-associated speck-like protein (ASC) and caspase 1 [12]. The inflammasome provides the platform to activate caspase 1 by autoproteolytic cleavage of pro-caspase-1 to generate the two fragments (i.e., p20 and p10) which forms a tetrameric form of the active caspase-1 that mediates pro-inflammatory cytokines maturation [13,14]. Several types of inflammasomes have been identified involving different sensors/receptors in the NOD-like receptor (NLR) family that initiates the assembly of the complex, among which the NLRP3 inflammasome is the best studied and implicated in AD pathogenesis [12,15]. The inflammasome components, such as NLRP1, NLRP3, ASC, caspase-1, as well as downstream effectors, such as IL-1β and IL-18, are upregulated in AD patients both in mRNA level [16] and protein level [15]. NLRP3 inflammasome serves as a sensor of Aβ fibrils and mediates the recruitment of microglia to exogenous Aβ in the brain [17]. More importantly, genetic studies using *Nlrp3*$^{-/-}$ or *Casp1*$^{-/-}$ mice demonstrated that NLRP3 inflammasome deficiency protects APP/PS1 mice from loss of cognitive function and reduced amyloid deposition [15]. A similar genetic study demonstrated that ASC haplodeficiency also rescued spatial reference memory deficits and amyloid plaque loads in 5xFAD mice [18]. These studies strongly suggest that NLRP3 inflammasome inhibition represents a new therapeutic target for AD.

Recently, we have developed small molecule and selective NLRP3 inhibitors [19]. Our prior studies demonstrated that the most potent one, JC-124, inhibits the formation of NLRP3 inflammasomes and the activation of caspase-1, and suppresses the production of IL-1β both *in vitro* and *in vivo* with beneficial effects in ischemic models [19]. In a separate study (not shown), we found significant levels of JC-124 in the brain tissues 1 hour after oral administration, suggesting that JC124 is a BBB penetrant. Herein, we report the rescuing effects of this new NLRP3 inflammasome inhibitor in the CRND8 APP Tg mouse model.

METHODS AND MATERIALS

Animals and JC-124 treatment

CRND8 mice (n = 8, half male and half female, 9 months old) carrying the AβPP695 gene with double mutations at KM670/671/NL (Swedish mutation), along with V717F (Indiana

mutation) on a C3H/He-C57BL/6 background were used in this study. The CRND8 mice were obtained from University of Toronto under a MTA and maintained at Case Western Reserve University. As a widely used AD mouse model, CRND8 mice demonstrate behavioral deficit along with Thioflavine S-positive Aβ deposit at 3 months of age and dense core plaques and neuritic pathology apparent at 5–6 months[20]. Other pathological changes such as increased oxidative stress, neuroinflammation and synaptic abnormalities were also reported in this model [21,22].

All animals were group housed and provided ad libitum access to food and water and maintained on a 12-hour light/dark cycle. All animals were treated following approved protocols by The Institutional Animal Care and Use Committee (IACUC) of Case Western Reserve University and experimental groups (JC-124 treated or vehicle treated) were determined in a random fashion matched with gender. JC-124 was dissolved in poly (ethylene glycol) BioUltra 400 (SIGMA Aldrich 91893). Body weight, appetite, and behavior after injection were closely monitored. Experimental animals were administered either vehicle or JC-124 (50 mg/kg/day) by intraperitoneal injection. Mice were treated five times per week for 4 consecutive weeks. One JC-124 treated-male mouse died during treatment.

Tissue collection

After injection for 4 weeks, mice were sacrificed. The brains were carefully removed, and the hemispheres were separated. Right hemispheres were fixed in 4% paraformaldehyde for immunohistochemical analyses, and the cortex and hippocampus were dissected from the left hemispheres, frozen on dry ice and stored at −80°C for biochemical studies. Brain tissue for immunohistochemistry was embedded in paraffin and sectioned with a microtome. 25 slides with 4 sagittal sections (6 μm) on each slide containing the hippocampus and cortical regions were cut and slides were numbered in order and used for quantitative analysis.

Immunohistochemistry

Paraffin sections were deparaffinized in xylene and rehydrated by serially dipping into 100%, 95%, 70%, 50% ethanol to PBS. Antigen retrieval through pressure cooking was used for some experiments (Biocare Medical, Concord, MA, USA). The slides were blocked for 30 min in 10% normal goat serum (NGS) in PBS and then sections were incubated overnight at 4°C with the following primary antibodies: anti-caspase-1 p10 (1:100, Santa Cruz Biotechnology, Santa Cruz, CA, USA), anti-amyloid oligomers (NU-2, 1:2000 [23]), anti-amyloid 1–16 (82E1, 1:250, Immunobiological Laboratories, Minneapolis, MN, USA), anti-Iba-1 (1:250, Wako, Osaka, Japan), anti-HNE (1:100, Alpha Diagnostics Intl. Inc., San Antonio, TX, USA) and anti-GFAP (1:100, Invitrogen, Carlsbad, CA, USA). Species-specific secondary antibodies and PAP complexes were added in sequence for 30 min and 1 h, then visualized with diaminobenzidine (DAB, Dako). Some sections were counterstained with hematoxylin staining, for 3 min followed by dip in acid alcohol. Slides were dehydrated through ascending ethanol to xylene, and then coverslipped. Double staining was also used for some experiments with one antibody detected with DAB-peroxidase method and the second antibody detected with FastBlue using the alkaline phosphatase method as we

previously described [24]. Brain sections were visualized using Zeiss Axiophot system and images were obtained with Zeiss Axiovision.

Aβ plaque quantification

To quantify the amyloid plaque burden in cerebral cortex and hippocampus areas, a total of 5 sections approximately 140 μm apart, starting with the first section in which the hippocampus was visible, were immunostained with the NU2 and 82E1 antibodies. For image analysis, the cortex was imaged using a 1.25X objective and the hippocampus was imaged using a 5X objective. The percent area immunostained was quantified using Axiovision image analysis software (Zeiss) under the same conditions and at the same time.

Microglia activation state classification

Microglia activation state was determined using parameters of size, shape, and number of branches as outlined previously [25]. To quantify the number of plaques invaded with different types of microglia, the large cortical plaques at least 50 μm in diameter (at least n-10 per animal) were analyzed with the genotype blinded to technician. The total number of microglia in the cortex were quantified using the Axiovision image analysis software (Zeiss).

Aβ ELISA

Hippocampus tissues were sequentially homogenized in TBS, in 1% Triton X-100 in TBS (TBS-TX buffer), and then in 5M Guandine-HCl in TBS, with all the homogenization buffers containing 1X Protease Inhibitors and 1X phosphatase Inhibitors (Roche Diagnostics). After homogenization, samples in TBS and TBS-TX buffer were centrifuged at 17,500 g for 30 min at 4°C and samples in Guandine-HCl were centrifuged at 16,000 g for 30 min at 4°C. The supernatants were collected at each step for ELISA and pellets were used for subsequent extraction steps. Human $A\beta_{42}$ ELISA Kit (Invitrogen) was used.

Western blotting assay

Dissected cortices were homogenized in cell lysis buffer (Cell Signaling Technology, Danvers, MA, USA) with added phosphatase inhibitors, protease inhibitors (Roche) and PMSF (1 mM). After homogenates were centrifuged at 18 000 rcf for 15 min at 4°C, the supernatants were collected and stored at −80°C. Proteins (20 μg per lane) were separated by electrophoresis on polyacrylamide gels (SDS-PAGE) and transferred onto polyvinylidene difluoride membranes (Millipore Corporation, Billerica, MA, USA) for western blotting as previously described [26]. After blocking with 10% nonfat milk in Tris-buffered saline (TBS) with 0.1% Tween 20 (TBS-T), proteins were probed with primary antibodies overnight at 4°C: anti-NLRP3 (1:500, Novus Biologicals, Littleton, CO, USA), anti-ASC (1:1000, Novus Biologicals), anti-caspase-1 (1:1000, Cell Signaling Technology, Danvers, MA, USA), 22C11 (1:2000, Millipore, Billerica, MA, USA), 82E1 (1:2000, Immunobiological Laboratories, Minneapolis, MN, USA), HO-1 (1:1000, Enzo Life Sciences, NY, USA), GFAP (1:1000, Santa Cruz Biotechnology, Santa Cruz, CA, USA), synaptophysin (1:5000, Abcam, Cambridge, UK) and GAPDH (1:10000, Cell Signaling Technologies). Then, the blots were rinsed in TBS-T and the proteins of interest were

applied with HRP-labeled rabbit or mouse secondary antibodies at 1:10000 dilution (Cell Signaling Technology, Danvers, MA, USA). After rinsing in TBS-T, membranes were incubated in a luminol reagent (Santa Cruz Biotechnology, Santa Cruz, CA, USA), and developed on X-ray film. The density of each immunoreactive band was measured using Image J software program (http://imagej.nih.gov/ij/). GAPDH levels were used as internal loading control.

Statistical analysis

All values were expressed as mean±SEM of each samples. Samples were analyzed using Student's *t* test. $P < 0.05$ was considered statistically significant.

RESULTS

NLRP3 inflammasome signaling pathway is activated in TgCRND8 mice

We first determined whether NLRP3 inflammasome signaling pathway is activated in the brain of CRND8 APP transgenic mice by examining the expression of NLRP3, ASC and cleavage of caspase 1. Western blot analysis of cortical homogenates revealed that expression of NLRP3 and ASC is significantly increased in TgCRND8 mice compared to non-Tg littermate controls ($P<0.05$; Fig. 1A–C). More importantly, while pro-caspase 1 levels remained unchanged, significantly increased amounts of cleaved caspase 1 (p20) was observed in the cortical lysates from TgCRND8 mice compared with that from non-Tg littermate controls ($P<0.01$; Fig. 1A, D). Immunohistochemical staining with antibody recognizing cleaved caspase-1 p10 was also performed. Diffusive staining with tiny granular structures was often noted in both neurons and glial cells in the cortex and hippocampus of non-Tg control mouse. Some cells contained more than two, often relatively smaller, granules. Interestingly, much larger granules with more intensive immunostaining, usually one to two per cell, were found in the perinuclear area in many neurons and glial cells in TgCRND8 mouse brain (Fig. 1E). Quantification revealed that the average size of p10-positive granules in the TgCRND8 mice was significantly larger than that in the non-Tg littermate control mice ($P<0.001$; Fig. 1F).

JC-124 inhibits the NLRP3 signaling in TgCRND8 mice

We previously demonstrated that JC-124 selectively inhibits the NLRP3 inflammasome signaling and limits infarct size following myocardial ischemia/reperfusion *in vivo* [19]. Given that we demonstrated the activation of NLRP3 inflammasome in the TgCRND8 mice, we next determined whetherJC-124 could inhibit NLRP3 inflammasome signaling and exert protective effects in these mice. 9-month-old TgCRND8 mice were treated with JC-124 (50 mg/kg daily, i.p. injection) for one month. Western blot analysis of cortical homogenates demonstrated significantly reduced levels of cleaved caspase-1 in JC-124 treated TgCRND8 mice compared with the TgCRND8 mice without treatment ($P<0.05$; Fig. 2A, B), confirming that JC-124 treatment led to inhibition of NLRP-3 inflammasome signaling in the brain of TgCRND8 mice. Consistently, immunohistochemical staining with antibody against cleaved caspase-1 p10 demonstrated that the average size of the p10-positive granules was also significantly reduced in the brain of TgCRND8 mice treated with JC-124 ($P<0.05$; Fig. 2C, D).

JC-124 decreases Aβ deposition in TgCRND8 mice

In the brain of TgCRND8 mice, amyloid plaques begin to form at 3 months of age and become readily observed after six months of age and continue to increase with aging [20]. To assess the effects of JC-124 on Aβ deposition, immunohistochemical study using the 82E1 antibody against the Aβ residue 1–16 was performed (Fig. 3A, top). Abundant large amyloid plaques were present in the cortex (Fig. 3A) and hippocampus (not shown) of TgCRND8 mice without JC-124 treatment, while much smaller and fewer amyloid plaques were found in the TgCRND8 mice treated with JC-124. Quantification of area occupied by the amyloid plaques as an index for amyloid load confirmed a significant reduction in amyloid deposition ($P < 0.05$; Fig. 3B) and a significant decrease in the average size of the amyloid plaques ($P < 0.01$; Fig. 3C) in TgCRND8 mice after JC-124 treatment. It is believed that oligomeric Aβ plays an important pathogenic role in AD. We further measured the effect of JC-124 on the accumulation of oligomeric Aβ by utilizing the NU2 antibody that specifically detects Aβ oligomers (Fig. 3A, bottom). We found that JC-124 treatment also led to significantly reduced Aβ oligomer deposition in the cortex and hippocampus ($P < 0.05$; Fig. 3D and $P < 0.001$; Fig. 3E).

JC-124 reduces β-cleavage of APP and Aβ production

The level of Aβ, especially $A\beta_{1–42}$, is essential to the process of amyloid deposition in AD. To complement our immunohistochemical analysis, we determined the levels of TBS-soluble, TBS-Triton X-100 (TBS-TX)-soluble and GuHCl-extracted $A\beta_{1–42}$ in the CRND8 mouse brain by ELISA. The aggregated $A\beta_{1–42}$ is dissolvable in GuHCl and $A\beta_{1–42}$ in GuHCl extracts of brain are strongly associated with amyloid burden visualized by immunohistochemistry [27]. Consistent with the observation of reduced amyloid plaque loads after JC-124 treatment, $A\beta_{1–42}$ content in GuHCl extracts was significantly reduced in TgCRND8 mice treated with JC-124 ($P < 0.05$; Fig. 4C). The levels of soluble $A\beta_{1–42}$ in both the TBS and TBS-TX extracts were also significantly reduced in the TgCRND8 mice after JC-124 treatment ($P < 0.05$; Fig. 4A, B), suggesting likely changes in Aβ production and/or clearance.

Aβ is produced by the sequential β-secretase and γ-secretase proteolytic cleavage of Aβ precursor protein (APP) [28], and β-C-terminal fragment of APP (β-CTF) is the product of β-secretase cleavage [28,29]. Western blot analysis of cortical homogenates demonstrated that the levels of full length APP was not affected by the treatment of JC-124 (Fig. 4E). However, the levels of β-CTF were reduced in the TgCRND8 mice treated with JC-124 ($P = 0.05$; Fig. 4F). These data indicated that JC-124 treatment caused reduced cleavage of APP by β-secretase.

JC-124 reduces microgliosis but increases astrocytosis in TgCRND8 mice

It was suggested that NLRP3 inflammasome signaling pathway enhances AD progression by mediating a harmful inflammatory tissue response. Microglia are the resident inflammatory cells in the brain, are highly activated in the brain of AD patients [30,31] and animal models [32,33] and are widely examined as a neuroinflammation marker for AD research [34]. We therefore examined the number and activation state of microglia by immunohistochemistry using Iba1 antibody (Fig. 5A). The total number of Iba-1 positive microglia was

significantly decreased in the TgCRND8 mice treated with JC-124 ($P < 0.05$; Fig. 5B). Interestingly, we found that in the vehicle-treated CRND8 mice, NU2-positive plaques are closely associated with type III/IV microglia which are the more activated glial cell types (Fig. 5A). However, JC-124 treatment decreased the plaques associated with type III/IV microglial cells but increased the population of plaques associated only with less active Type I/II microglia ($P = 0.13$; Fig. 5C). Collectively, these data supported that JC-124 reduced microglial-dependent tissue inflammatory response.

Astrocytes are also involved in inflammatory response and phagocytosis [35,36], we then used a GFAP antibody, a sensitive and reliable marker that labels most reactive astrocytes that are responding to CNS injuries. Western blot of cortical homogenates demonstrated a significant increase in the expression of GFAP in the brain of TgCRND8 mice treated with JC-124 compared to those without treatment ($P < 0.05$; Fig. 6A, B). Consistent with the western blot data, immunohistochemical analysis also revealed significantly increased astrocytosis quantified by the area stained ($P < 0.05$; Fig. 6C, D). Collectively, these data demonstrated that JC-124 treatment caused increased astrocytosis in TgCRND8 mice.

JC-124 reduces oxidative stress in TgCRND8 mice after long-term treatment

Oxidative stress is a prominent early feature in AD [37] and closely correlates with inflammasome formation and inflammation [38,39]. Furthermore, activated microglia can promote the release of reactive oxygen species (ROS). To determine whether JC-124 has protective effects on oxidative stress in TgCRND8 mice, two widely used oxidative stress markers in AD models, namely HO-1 and HNE, were measured. Notably, treatment of TgCRND8 mice with JC-124 significantly reduced the level of HO-1 ($P < 0.05$; Fig. 7A, B), an inducible isoform in response to oxidative stress. JC-124 treatment also resulted in a decrease of neuronal HNE level ($P = 0.0971$; Fig. 7C, D), a marker of lipid peroxidation. These results suggested that JC-124 treatment reduced oxidative stress in the TgCRND8 mice.

Treatment of TgCRND8 mice with JC-124 improves the level of synaptic marker

Synaptic dysfunction is an early event in AD patients, correlates well with cognitive impairment during the course of disease [40]. To evaluate the effects of JC-124 on synaptic pathology, we examined the levels of synaptophysin (Fig. 8A), a presynaptic marker. There was significantly increased levels of synaptophysin expression in the TgCRND8 mice treated with JC-124 compared with those without JC-124 treatment ($P < 0.05$; Fig. 8B), suggesting a synaptoprotective effect of JC-124 in the TgCRND8 mice.

DISCUSSION

Previous genetic studies suggested that inhibition of NLRP3 inflammasome signaling pathway is a potential therapeutic target for AD. Indeed, two most recent studies demonstrated promising neuroprotective effects of fenamate NSAIDs and MCC950 as NLRP3 inflammasome inhibitors in AD mouse models [41,42]. The major purpose of this study was to test whether a selective NLRP3 inhibitor that we recently developed could rescue the AD-associated deficits in an AD animal model. In this study, we used the CRND8

APP transgenic mouse model which develops AD-relevant pathological deficits. We first demonstrated that NLRP3 signaling pathway is activated in CRND8 APP Tg mice as evidenced by the increased expression of NLRP3 and ASC as well as increased cleavage of caspase 1 compared with non-Tg littermate controls. This is consistent with prior studies demonstrating extensive caspase-1 cleavage and activation in human patients with mild cognitive impairment and with AD, as well as in the brain of APP/PS1 transgenic model [15], thus making TgCRND8 mouse a suitable model to study the effects of NLRP3 inflammasome inhibition on AD-related deficits. One-month treatment of JC-124, a selective inflammasome inhibitor, of the TgCRND8 mice indeed reduced caspase-1 cleavage and activation. Importantly, JC-124 treatment led to alleviation of AD-associated deficits such as reduced amyloid pathology, reduced microgliosis, and oxidative stress, and increased synaptic markers and astrocytosis in the TgCRND8 mice, thus supporting the further development of NLRP3 inflammasome inhibitors as a viable option for AD therapeutics.

Compared with prior genetic studies [15,18], there are several important aspects of our study to be noted. Of course, the common major finding is that inhibition of NLRP3 inflammasome either by genetic deficiency such as that published in the prior studies [15,18] or by pharmaceutical methods such as being demonstrated here resulted in decreased Aβ deposition and positively impacted other AD-relevant deficits in AD mouse models. The reduced amyloid deposition could be due to reduced Aβ production, aggregation and/or increased clearance. Although both studies demonstrated significantly reduced levels of Aβ after NLRP3 inflammasome inhibition, no significant changes in the production of β-CTF were seen in APP/PS1/Nlrp$^{-/-}$ compared with APP/PS1 mice [15], suggesting that Aβ production is not affected in this genetic inhibition study and instead the authors suggested enhanced clearance. However, we demonstrated reduced β-CTF production in the TgCRND8 mice treated with JC-124, suggesting that the effects of JC-124 on reduced plaque loads also involves reduced β-cleavage of APP and reduced Aβ production. While it remains to be determined whether JC-124 directly inhibits β-secretase activity, it is possible that JC-124 reduces β-secretase activity through reduced inflammatory response since proinflammatory cytokines are known to potentiate BACE1 expression and activity through PPARγ depletion [43] and inflammation inhibition led to reduced BACE1 activity [44]. Since Aβ aggregation and plaque formation are enhanced in the condition of inflammatory response through nitrating Aβ at tyrosine 10 by nitric oxide [45], reduced inflammation and oxidative stress could contribute to the reduced Aβ deposition in both studies.

One important distinction between the prior genetic inhibition study and the current pharmaceutical inhibition study is that the genetic studies involves NLRP3 inhibition since the mouse was born while our study began the treatment since 9 months of age. At this age, TgCRND8 mice have developed extensive amyloid pathology. Therefore, our treatment regimen closely mimicked the likely treatment scheme with AD patients that already developed amyloid pathology. We thus demonstrated that inhibition of NLRP3 inflammasome pathway even at a relatively later point in the progression of amyloidosis is still effective in reversing the accumulation of amyloid pathology and positively impacting other AD-relevant deficits such as alleviation of oxidative stress and enhancement of synaptogenesis.

Another important distinction is the differential effects on microgliosis and astrocytosis. In the genetic inhibition studies, microglia mediated phagocytosis was significantly increased in APP/PS1/Nlrp$^{-/-}$ and APP/PS1/Casp1$^{-/-}$ mice compare to APP/PS1 mice which was suggested to be the major clearance pathway that leads to reduced Aβ levels and amyloid loads [15]. However, in our study, the total number of Iba-1 positive microglial cells were decreased and also those microglia associated with plaques became less activated in the TgCRND8 mice after JC-124 treatment. Interestingly, in the two most recent study using fenamate NSAIDs or MCC950 as NLRP3 inhibitors to treat mouse models of AD, active microglial cells were also reduced by the treatment in AD mouse models [41,42]. These data suggest that microglia-mediated phagocytosis is unlikely activated and responsible for amyloid plaque reduction in JC-124 treated TgCRND8 mice. Instead, we found significantly increased expression of GFAP and increased astrocytosis in the TgCRND8 mice after JC-124 treatment. The role of astrocytosis in the pathogenesis of AD remains controversial. Some evidences suggest that astrocytes contribute to enhanced neuroinflammation and potentiate the pathogenesis of AD while other demonstrated that astrocytosis may contribute to degradation of plaques. For example, astrocytes express high level of IL-23 receptor and uptake of Aβ by astrocytes may be enhanced by microglia-derived IL-12 p40 [46]. Adult mouse astrocytes have been shown to bind and degrade Aβ in brain sections from a human APP-expressing mouse model [35], and astrocytes transplants internalized Aβ in APPswe/PS1dE9 mice [47]. Astrocytes have also been shown to impact Aβ by indirect mechanism such as by releasing lapidated apolipoprotein E and enhancing microglia phagocytosis of Aβ [36]. Importantly, a very recent study demonstrated that downregulation of inflammasome activity via ASC heterozygous expression increased phagocytosis in astrocytes *in vitro* and decreased amyloid load *in vivo* [18]. Our observation of significantly enhanced astrocytosis in the TgCRND8 mice after JC-124 treatment accompanied by decreased amyloid burden is consistent with the observation in ASC heplodeficiency study that appears to suggest the involvement of enhanced astrocytosis as a major clearance mechanism to degrade and reduce amyloid plaques in the brain after NLRP3 inflammasome inhibition.

Synapse loss is the major pathology correlated to cognitive decline in AD [48,49]. Synaptic plasticity is sensitive to IL-1β, and IL-1β has been demonstrated to disrupt the formation of dendritic spines, leading to the inhibition of BDNF-dependent LTP through reducing TrkB-mediated BDNF signaling and the activation of p38 [50]. In this regard, it is of interest to note that, in our study, JC-124 treated TgCRND8 mice demonstrated significantly increased synaptophysin expression, likely through better preservation of synaptic plasticity due to presumably reduced IL-1β via NLRP3 inflammasome inhibition by JC-124. Consistent with the notion of better preserved synaptic plasticity after inflammasome inhibition, deficiency of NLRP3 or caspase-1 has been shown to lead to a complete protection from Aβ-induced suppression of memory and behavior in APP/PS1 mice [15]. Ablation of NLRP3 even ameliorated the age-related memory deficiency in the mice without experimental brain amyloidosis [51].

In summary, in this study we demonstrated that treatment with JC-124, a small molecule NLRP3 inflammasome inhibitor, inhibits the caspase-1 cleavage and activation in the TgCRND8 mice which effectively reduced amyloid deposition and alleviated AD-associated

deficits. Our results demonstrated that further development and characterization of NLRP3 inflammasome inhibitors as potential therapeutic agents for AD are warranted.

Acknowledgments

The work was supported in part by the National Institute on Aging of the National Institutes of Health [RFAG049479 to X.Z. and R01AG041161 to S.Z.]; Alzheimer's Association [AARG-16-443584 to X.Z.]; Dr. Robert M. Kohrman Memorial Fund to X.Z., Alzheimer's Drug Discovery Foundation [20150601 to S.Z.]; and the National Natural Sciences Foundation of China [81100594 to J.Y.].

References

1. Selkoe DJ. Alzheimer's disease: genes, proteins, and therapy. Physiol Rev. 2001; 81(2):741–766. [PubMed: 11274343]
2. Selkoe DJ, Hardy J. The amyloid hypothesis of Alzheimer's disease at 25 years. EMBO Mol Med. 2016; 8(6):595–608. [PubMed: 27025652]
3. Strandberg TE, Tilvis RS. C-reactive protein, cardiovascular risk factors, and mortality in a prospective study in the elderly. Arterioscler Thromb Vasc Biol. 2000; 20(4):1057–1060. [PubMed: 10764673]
4. Swardfager W, Lanctot K, Rothenburg L, Wong A, Cappell J, Herrmann N. A meta-analysis of cytokines in Alzheimer's disease. Biol Psychol. 2010; 68(10):930–941.
5. Lim SL, Rodriguez-Ortiz CJ, Kitazawa M. Infection, systemic inflammation, and Alzheimer's disease. Microbes Infect. 2015; 17(8):549–556. DOI: 10.1016/j.micinf.2015.04.004 [PubMed: 25912134]
6. Weggen S, Eriksen JL, Das P, Sagi SA, Wang R, Pietrzik CU, Findlay KA, Smith TE, Murphy MP, Bulter T, Kang DE, Marquez-Sterling N, Golde TE, Koo EH. A subset of NSAIDs lower amyloidogenic Abeta42 independently of cyclooxygenase activity. Nature. 2001; 414(6860):212–216. [PubMed: 11700559]
7. Sastre M, Dewachter I, Landreth GE, Willson TM, Klockgether T, van Leuven F, Heneka MT. Nonsteroidal anti-inflammatory drugs and peroxisome proliferator-activated receptor-gamma agonists modulate immunostimulated processing of amyloid precursor protein through regulation of beta-secretase. J Neurosci. 2003; 23(30):9796–9804. [PubMed: 14586007]
8. McGeer PL, McGeer EG. The amyloid cascade-inflammatory hypothesis of Alzheimer disease: implications for therapy. Acta Neuropathol. 2013; 126(4):479–497. [PubMed: 24052108]
9. Heneka MT, O'Banion MK, Terwel D, Kummer MP. Neuroinflammatory processes in Alzheimer's disease. J Neural Transm (Vienna). 2010; 117(8):919–947. [PubMed: 20632195]
10. Korvatska O, Leverenz JB, Jayadev S, McMillan P, Kurtz I, Guo X, Rumbaugh M, Matsushita M, Girirajan S, Dorschner MO, Kiianitsa K, Yu CE, Brkanac Z, Garden GA, Raskind WH, Bird TD. R47H variant of TREM2 associated with Alzheimer disease in a large late-onset family: clinical, genetic, and neuropathological study. JAMA Neurol. 2015; 72(8):920–927. DOI: 10.1001/jamaneurol.2015.0979 [PubMed: 26076170]
11. Jonsson T, Stefansson H, Steinberg S, Jonsdottir I, Jonsson PV, Snaedal J, Bjornsson S, Huttenlocher J, Levey AI, Lah JJ, Rujescu D, Hampel H, Giegling I, Andreassen OA, Engedal K, Ulstein I, Djurovic S, Ibrahim-Verbaas C, Hofman A, Ikram MA, van Duijn CM, Thorsteinsdottir U, Kong A, Stefansson K. Variant of TREM2 associated with the risk of Alzheimer's disease. N Engl J Med. 2013; 368(2):107–116. DOI: 10.1056/NEJMoa1211103 [PubMed: 23150908]
12. Freeman LC, Ting JP. The pathogenic role of the inflammasome in neurodegenerative diseases. J Neurochem. 2016; 136(Suppl 1):29–38. DOI: 10.1111/jnc.13217 [PubMed: 26119245]
13. Schroder K, Tschopp J. The inflammasomes. Cell. 2010; 140(6):821–832. [PubMed: 20303873]
14. Shao BZ, Xu ZQ, Han BZ, Su DF, Liu C. NLRP3 inflammasome and its inhibitors: a review. Front Pharmacol. 2015; 6:262. [PubMed: 26594174]
15. Heneka MT, Kummer MP, Stutz A, Delekate A, Schwartz S, Vieira-Saecker A, Griep A, Axt D, Remus A, Tzeng TC, Gelpi E, Halle A, Korte M, Latz E, Golenbock DT. NLRP3 is activated in

Alzheimer's disease and contributes to pathology in APP/PS1 mice. Nature. 2013; 493(7434):674–678. DOI: 10.1038/nature11729 [PubMed: 23254930]

16. Saresella M, La Rosa F, Piancone F, Zoppis M, Marventano I, Calabrese E, Rainone V, Nemni R, Mancuso R, Clerici M. The NLRP3 and NLRP1 inflammasomes are activated in Alzheimer's disease. Mol Neurodegener. 2016; 11:23. [PubMed: 26939933]
17. Halle A, Hornung V, Petzold GC, Stewart CR, Monks BG, Reinheckel T, Fitzgerald KA, Latz E, Moore KJ, Golenbock DT. The NALP3 inflammasome is involved in the innate immune response to amyloid-beta. Nat Immunol. 2008; 9(8):857–865. [PubMed: 18604209]
18. Couturier J, Stancu IC, Schakman O, Pierrot N, Huaux F, Kienlen-Campard P, Dewachter I, Octave JN. Activation of phagocytic activity in astrocytes by reduced expression of the inflammasome component ASC and its implication in a mouse model of Alzheimer disease. J Neuroinflammation. 2016; 13:20. [PubMed: 26818951]
19. Marchetti C, Toldo S, Chojnacki J, Mezzaroma E, Liu K, Salloum FN, Nordio A, Carbone S, Mauro AG, Das A, Zalavadia AA, Halquist MS, Federici M, Van Tassell BW, Zhang S, Abbate A. Pharmacologic inhibition of the NLRP3 inflammasome preserves cardiac function after ischemic and nonischemic injury in the mouse. J Cardiovasc Pharmacol. 2015; 66(1):1–8. DOI: 10.1097/FJC.0000000000000247 [PubMed: 25915511]
20. Chishti MA, Yang DS, Janus C, Phinney AL, Horne P, Pearson J, Strome R, Zuker N, Loukides J, French J, Turner S, Lozza G, Grilli M, Kunicki S, Morissette C, Paquette J, Gervais F, Bergeron C, Fraser PE, Carlson GA, George-Hyslop PS, Westaway D. Early-onset amyloid deposition and cognitive deficits in transgenic mice expressing a double mutant form of amyloid precursor protein 695. J Biol Chem. 2001; 276(24):21562–21570. [PubMed: 11279122]
21. Ye H, Jalini S, Mylvaganam S, Carlen P. Activation of large-conductance Ca(2+)-activated K(+) channels depresses basal synaptic transmission in the hippocampal CA1 area in APP (swe/ind) TgCRND8 mice. Neurobiol Aging. 2010; 31(4):591–604. DOI: 10.1016/j.neurobiolaging.2008.05.012 [PubMed: 18547679]
22. Dudal S, Krzywkowski P, Paquette J, Morissette C, Lacombe D, Tremblay P, Gervais F. Inflammation occurs early during the Abeta deposition process in TgCRND8 mice. Neurobiol Aging. 2004; 25(7):861–871. DOI: 10.1016/j.neurobiolaging.2003.08.008 [PubMed: 15212840]
23. Velasco PT, Heffern MC, Sebollela A, Popova IA, Lacor PN, Lee KB, Sun X, Tiano BN, Viola KL, Eckermann AL, Meade TJ, Klein WL. Synapse-binding subpopulations of Abeta oligomers sensitive to peptide assembly blockers and scFv antibodies. ACS Chem Neurosci. 2012; 3(11):972–981. DOI: 10.1021/cn300122k [PubMed: 23173076]
24. Wang C, Zhang F, Jiang S, Siedlak SL, Shen L, Perry G, Wang X, Tang B, Zhu X. Estrogen receptor-alpha is localized to neurofibrillary tangles in Alzheimer's disease. Sci Rep. 2016; 6:20352.doi: 10.1038/srep20352 [PubMed: 26837465]
25. Gerenu G, Liu K, Chojnacki JE, Saathoff JM, Martinez-Martin P, Perry G, Zhu X, Lee HG, Zhang S. Curcumin/melatonin hybrid 5-(4-hydroxy-phenyl)-3-oxo-pentanoic acid [2-(5-methoxy-1H-indol-3-yl)-ethyl]-amide ameliorates AD-like pathology in the APP/PS1 mouse model. ACS Chem Neurosci. 2015; 6(8):1393–1399. [PubMed: 25893520]
26. Wang W, Wang X, Fujioka H, Hoppel C, Whone AL, Caldwell MA, Cullen PJ, Liu J, Zhu X. Parkinson's disease-associated mutant VPS35 causes mitochondrial dysfunction by recycling DLP1 complexes. Nat Med. 2016; 22(1):54–63. DOI: 10.1038/nm.3983 [PubMed: 26618722]
27. Shankar GM, Leissring MA, Adame A, Sun X, Spooner E, Masliah E, Selkoe DJ, Lemere CA, Walsh DM. Biochemical and immunohistochemical analysis of an Alzheimer's disease mouse model reveals the presence of multiple cerebral Abeta assembly forms throughout life. Neurobiol Dis. 2009; 36(2):293–302. DOI: 10.1016/j.nbd.2009.07.021 [PubMed: 19660551]
28. Li N, Liu K, Qiu Y, Ren Z, Dai R, Deng Y, Qing H. Effect of presenilin mutations on APP cleavage; insights into the pathogenesis of FAD. Front Aging Neurosci. 2016; 8:51. [PubMed: 27014058]
29. Barnwell E, Padmaraju V, Baranello R, Pacheco-Quinto J, Crosson C, Ablonczy Z, Eckman E, Eckman CB, Ramakrishnan V, Greig NH, Pappolla MA, Sambamurti K. Evidence of a novel mechanism for partial gamma-secretase inhibition induced paradoxical increase in secreted amyloid beta protein. PloS One. 2014; 9(3):e91531. [PubMed: 24658363]

30. McGeer PL, Itagaki S, Tago H, McGeer EG. Reactive microglia in patients with senile dementia of the Alzheimer type are positive for the histocompatibility glycoprotein HLA-DR. Neurosci Lett. 1987; 79(1–2):195–200. [PubMed: 3670729]

31. Styren SD, Civin WH, Rogers J. Molecular, cellular, and pathologic characterization of HLA-DR immunoreactivity in normal elderly and Alzheimer's disease brain. Exp Neurol. 1990; 110(1):93–104. [PubMed: 1698655]

32. Bellucci A, Westwood AJ, Ingram E, Casamenti F, Goedert M, Spillantini MG. Induction of inflammatory mediators and microglial activation in mice transgenic for mutant human P301S tau protein. Am J Pathol. 2004; 165(5):1643–1652. [PubMed: 15509534]

33. Janelsins MC, Mastrangelo MA, Oddo S, LaFerla FM, Federoff HJ, Bowers WJ. Early correlation of microglial activation with enhanced tumor necrosis factor-alpha and monocyte chemoattractant protein-1 expression specifically within the entorhinal cortex of triple transgenic Alzheimer's disease mice. J Neuroinflammation. 2005; 2:23. [PubMed: 16232318]

34. Heneka MT, Golenbock DT, Latz E. Innate immunity in Alzheimer's disease. Nat Immunol. 2015; 16(3):229–236. [PubMed: 25689443]

35. Wyss-Coray T, Loike JD, Brionne TC, Lu E, Anankov R, Yan F, Silverstein SC, Husemann J. Adult mouse astrocytes degrade amyloid-beta in vitro and in situ. Nat Med. 2003; 9(4):453–457. [PubMed: 12612547]

36. Terwel D, Steffensen KR, Verghese PB, Kummer MP, Gustafsson JA, Holtzman DM, Heneka MT. Critical role of astroglial apolipoprotein E and liver X receptor-alpha expression for microglial Abeta phagocytosis. J Neurosci. 2011; 31(19):7049–7059. [PubMed: 21562267]

37. Bonda DJ, Wang X, Lee HG, Smith MA, Perry G, Zhu X. Neuronal failure in Alzheimer's disease: a view through the oxidative stress looking-glass. Neurosci Bull. 2014; 30(2):243–252. DOI: 10.1007/s12264-013-1424-x [PubMed: 24733654]

38. Heneka MT, Kummer MP, Latz E. Innate immune activation in neurodegenerative disease. Nat Rev. 2014; 14(7):463–477.

39. Chen L, Na R, Boldt E, Ran Q. NLRP3 inflammasome activation by mitochondrial reactive oxygen species plays a key role in long-term cognitive impairment induced by paraquat exposure. Neurobiol Aging. 2015; 36(9):2533–2543. DOI: 10.1016/j.neurobiolaging.2015.05.018 [PubMed: 26119225]

40. Arendt T. Synaptic degeneration in Alzheimer's disease. Acta Neuropathol. 2009; 118(1):167–179. [PubMed: 19390859]

41. Dempsey C, Rubio Araiz A, Bryson KJ, Finucane O, Larkin C, Mills EL, Robertson AA, Cooper MA, O'Neill LA, Lynch MA. Inhibiting the NLRP3 inflammasome with MCC950 promotes non-phlogistic clearance of amyloid-beta and cognitive function in APP/PS1 mice. Brain Behav Immun. 2016; doi: 10.1016/j.bbi.2016.12.014

42. Daniels MJ, Rivers-Auty J, Schilling T, Spencer NG, Watremez W, Fasolino V, Booth SJ, White CS, Baldwin AG, Freeman S, Wong R, Latta C, Yu S, Jackson J, Fischer N, Koziel V, Pillot T, Bagnall J, Allan SM, Paszek P, Galea J, Harte MK, Eder C, Lawrence CB, Brough D. Fenamate NSAIDs inhibit the NLRP3 inflammasome and protect against Alzheimer's disease in rodent models. Na Commun. 2016; 7:12504.doi: 10.1038/ncomms12504

43. Sastre M, Dewachter I, Rossner S, Bogdanovic N, Rosen E, Borghgraef P, Evert BO, Dumitrescu-Ozimek L, Thal DR, Landreth G, Walter J, Klockgether T, van Leuven F, Heneka MT. Nonsteroidal anti-inflammatory drugs repress beta-secretase gene promoter activity by the activation of PPARgamma. Proc Natl Acad Sci U S A. 2006; 103(2):443–448. [PubMed: 16407166]

44. Kummer MP, Vogl T, Axt D, Griep A, Vieira-Saecker A, Jessen F, Gelpi E, Roth J, Heneka MT. Mrp14 deficiency ameliorates amyloid beta burden by increasing microglial phagocytosis and modulation of amyloid precursor protein processing. J Neurosci. 2012; 32(49):17824–17829. [PubMed: 23223301]

45. Kummer MP, Hermes M, Delekarte A, Hammerschmidt T, Kumar S, Terwel D, Walter J, Pape HC, Konig S, Roeber S, Jessen F, Klockgether T, Korte M, Heneka MT. Nitration of tyrosine 10 critically enhances amyloid beta aggregation and plaque formation. Neuron. 2011; 71(5):833–844. [PubMed: 21903077]

46. Vom Berg J, Prokop S, Miller KR, Obst J, Kalin RE, Lopategui-Cabezas I, Wegner A, Mair F, Schipke CG, Peters O, Winter Y, Becher B, Heppner FL. Inhibition of IL-12/IL-23 signaling reduces Alzheimer's disease-like pathology and cognitive decline. Nat Med. 2012; 18(12):1812–1819. [PubMed: 23178247]

47. Pihlaja R, Koistinaho J, Malm T, Sikkila H, Vainio S, Koistinaho M. Transplanted astrocytes internalize deposited beta-amyloid peptides in a transgenic mouse model of Alzheimer's disease. Glia. 2008; 56(2):154–163. [PubMed: 18004725]

48. Mucke L, Selkoe DJ. Neurotoxicity of amyloid beta-protein: synaptic and network dysfunction. Cold Spring Harb Perspect Med. 2012; 2(7):a006338. [PubMed: 22762015]

49. DeKosky ST, Scheff SW. Synapse loss in frontal cortex biopsies in Alzheimer's disease: correlation with cognitive severity. Ann Neurol. 1990; 27(5):457–464. [PubMed: 2360787]

50. Tong L, Prieto GA, Kramar EA, Smith ED, Cribbs DH, Lynch G, Cotman CW. Brain-derived neurotrophic factor-dependent synaptic plasticity is suppressed by interleukin-1beta via p38 mitogen-activated protein kinase. J Neurosci. 2012; 32(49):17714–17724. [PubMed: 23223292]

51. Youm YH, Grant RW, McCabe LR, Albarado DC, Nguyen KY, Ravussin A, Pistell P, Newman S, Carter R, Laque A, Munzberg H, Rosen CJ, Ingram DK, Salbaum JM, Dixit VD. Canonical Nlrp3 inflammasome links systemic low-grade inflammation to functional decline in aging. Cell Metab. 2013; 18(4):519–532. [PubMed: 24093676]

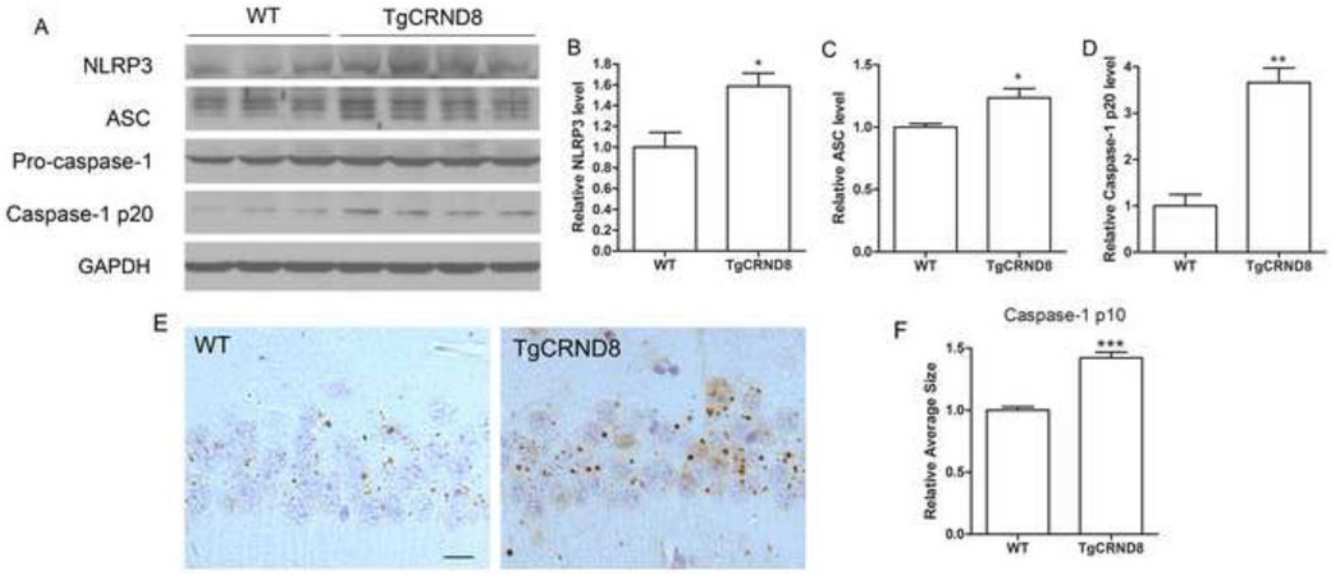

Figure 1. NLRP3 inflammasome activation in TgCRND8 mice

Representative western blot of cortical homogenates (**A**) and quantification analysis (**B–D**) revealed that the levels of NLRP3, ASC and cleaved caspase 1 (p20 cleavage product) were significantly increased in 10 months old CRND8 mice compared to non-transgenic WT littermate controls. GAPDH was used as an internal loading control. (**E**) Representative immunohistochemistry of caspase-1 p10 antibody (brown), a marker for activated capase-1, and sections counterstained with hematoxylin (blue). Scale bar represents 20 μm. (**F**) Images of the CA1 area of the hippocampus were analyzed by measuring the average size of caspase-1 p10-positive specks in pyramidal neurons which revealed significantly larger p10-positive specks in the CRND8 mice. Data represent mean ± SEM, Student's *t*-test, $*P < 0.05$, $**P < 0.01$, $***P < 0.001$.

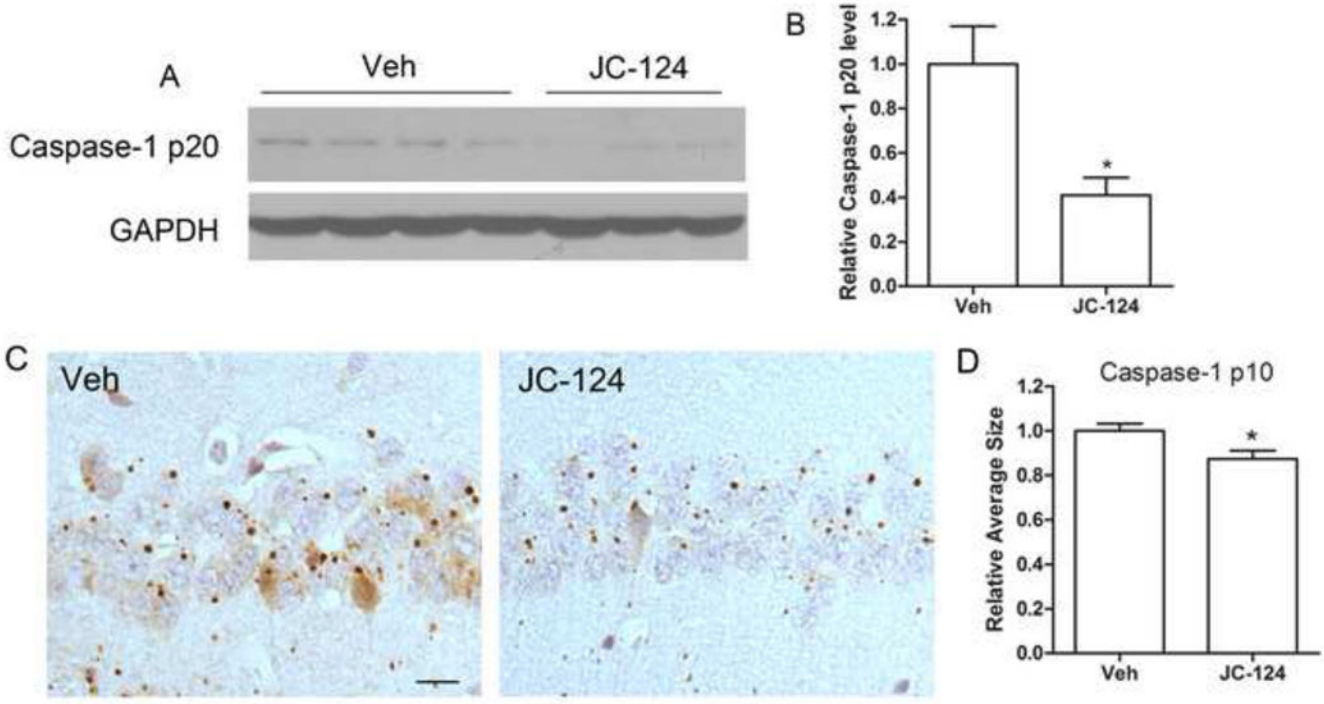

Figure 2. Effect of JC-124 on NLRP3 inflammasome activation in TgCRND8 mice

(**A**) Representative western blot of cortical homogenates (**A**) and quantification analysis (**B**) revealed that the levels of cleaved caspase 1 (p20 cleavage product) were significantly decreased in JC-124 treated CRND8 mice compared to vehicle-treated CRND8 mice. GAPDH was used as an internal loading control. (**C**) Representative immunohistochemistry of caspase-1 p10 antibody (brown) and sections counterstained with hematoxylin (blue) in the hippocampus of JC-124-treated and vehicle-treated CRND8 mice. Scale bar represents 20 μm. (**D**) Images of the CA1 area of the hippocampus were analyzed by measuring the average size of caspase-1 p10-positive specks in pyramidal neurons which revealed a significant decrease in the average size of these p10-positive specks in the JC-124-treated CRND8 mice compared to vehicle-treated CRND8 mice. Data represent mean ± SEM, Student's *t*-test, $*P < 0.05$.

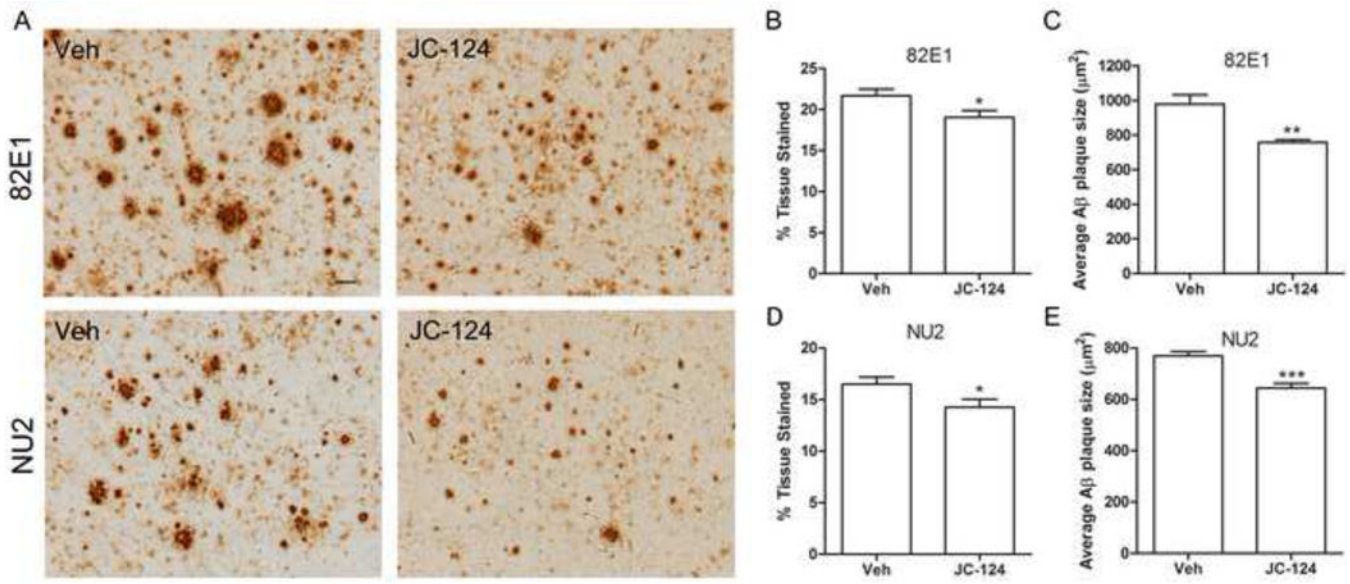

Figure 3. Effect of JC-124 on Aβ plaque load in TgCRND8 mice

(**A**) Representative immunohistochemistry of anti-$A\beta_{1-16}$ 82E1 antibody (upper) and anti-Aβ oligomer NU2 antibody (lower) in the cortex of JC-124 treated and vehicle treated CRND8 mice. Scale bar represents 50 μm. The amount of Aβ plaques were quantified as percent area tissue stained (**B, D**) and the average size of Aβ plaques was also quantified (**C, E**). Data represent mean ± SEM, Student's *t*-test, $*P < 0.05$, $**P < 0.01$, $***P < 0.001$.

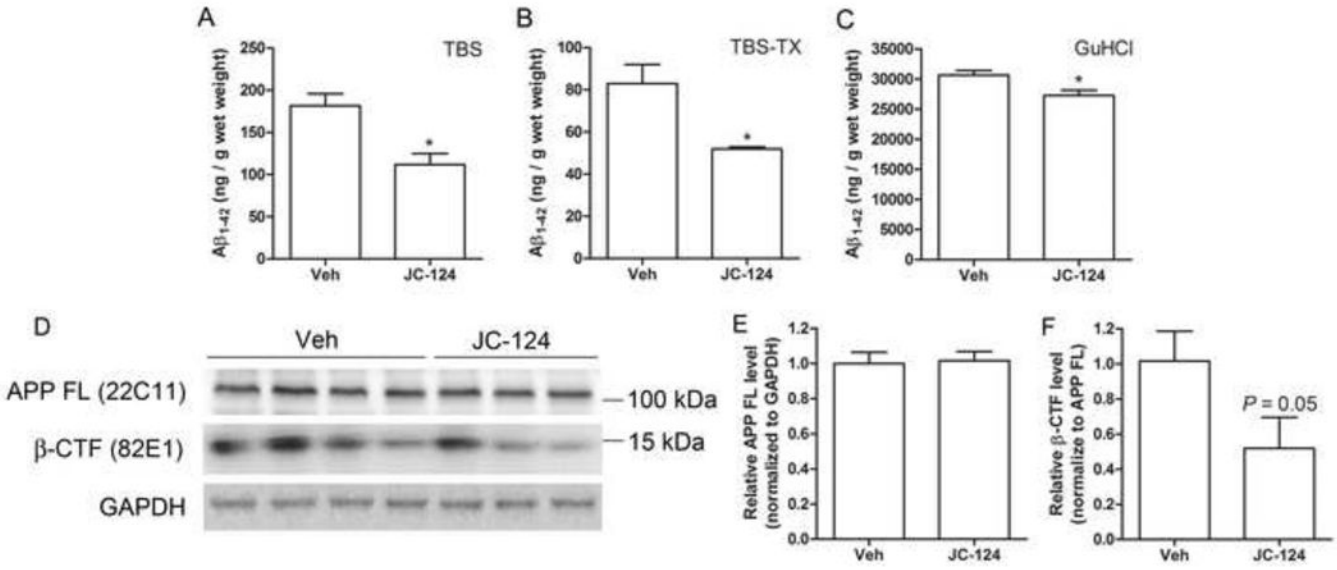

Figure 4. Effect of JC-124 on A$\beta_{1–42}$ and APP processing in TgCRND8 mice

(**A–C**) ELISA of A$\beta_{1–42}$ in the TBS, TBS Triton X-100 (TBS-TX) and Guandine-HCl (GuHCl) fractions of cortical tissues from vehicle- and JC-124-treated TgCRND8 mice. Representative western blot of cortical homogenates (**D**) and quantification analysis (**E**) revealed that no changes in the full length APP as detected by 22C11 antibody but decreased levels of β-CTF as detected by 82E1 (P=0.05, normalized to full length APP) in JC-124 treated CRND8 mice compared to vehicle-treated CRND8 mice. GAPDH was used as an internal loading control. Data represent mean ± SEM, Student's t-test, *$P < 0.05$.

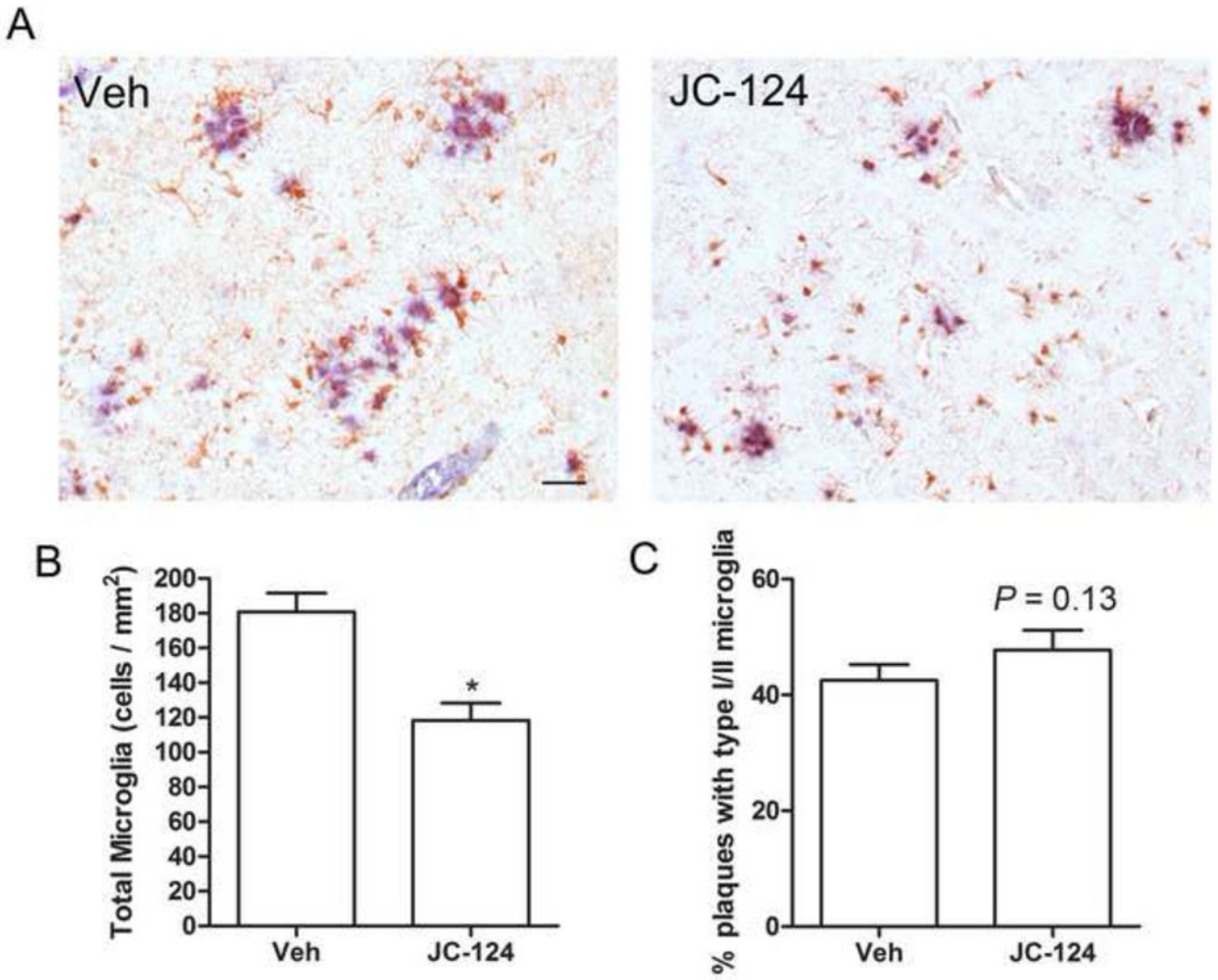

Figure 5. Effect of JC-124 on microgliosis in TgCRND8 mice

(**A**) Representative immunohistochemistry of anti-Iba-1 antibody (brown) and anti-Aβ oligomer antibody (blue) in the cortex of JC-124 treated and vehicle treated CRND8 mice. Scale bar represents 50 μm. (**B**) The total number of Iba-1-positive microglia was quantified as cell number per mm^2. (**C**) Percentage number of plaques associated with type I/II microglia was quantified. Data represent mean ± SEM, Student's *t*-test, $*P < 0.05$.

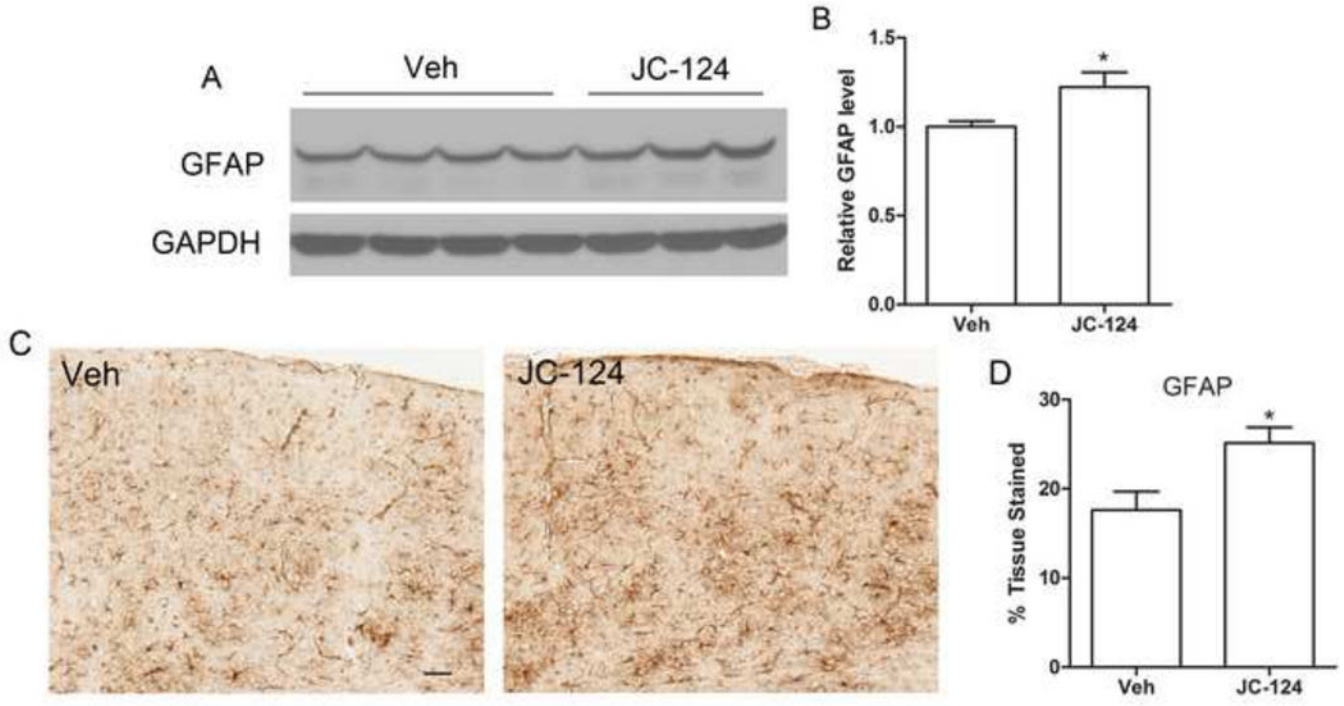

Figure 6. Effect of JC-124 on astrocytosis in TgCRND8 mice

Representative western blot of cortical homogenates (**A**) and quantification analysis (**B**) revealed that the levels of GFAP were significantly increased in JC-124-treated CRND8 mice compared to vehicle-treated CRND8 mice. GAPDH was used as an internal loading control. (**C**) Representative immunohistochemistry of anti-GFAP antibody in the cortex of JC-124 treated and vehicle treated CRND8 mice. Scale bar represents 50 μm. (**D**) % area stained by GFAP was quantified. Data represent mean ± SEM, Student's *t*-test, $*P < 0.05$.

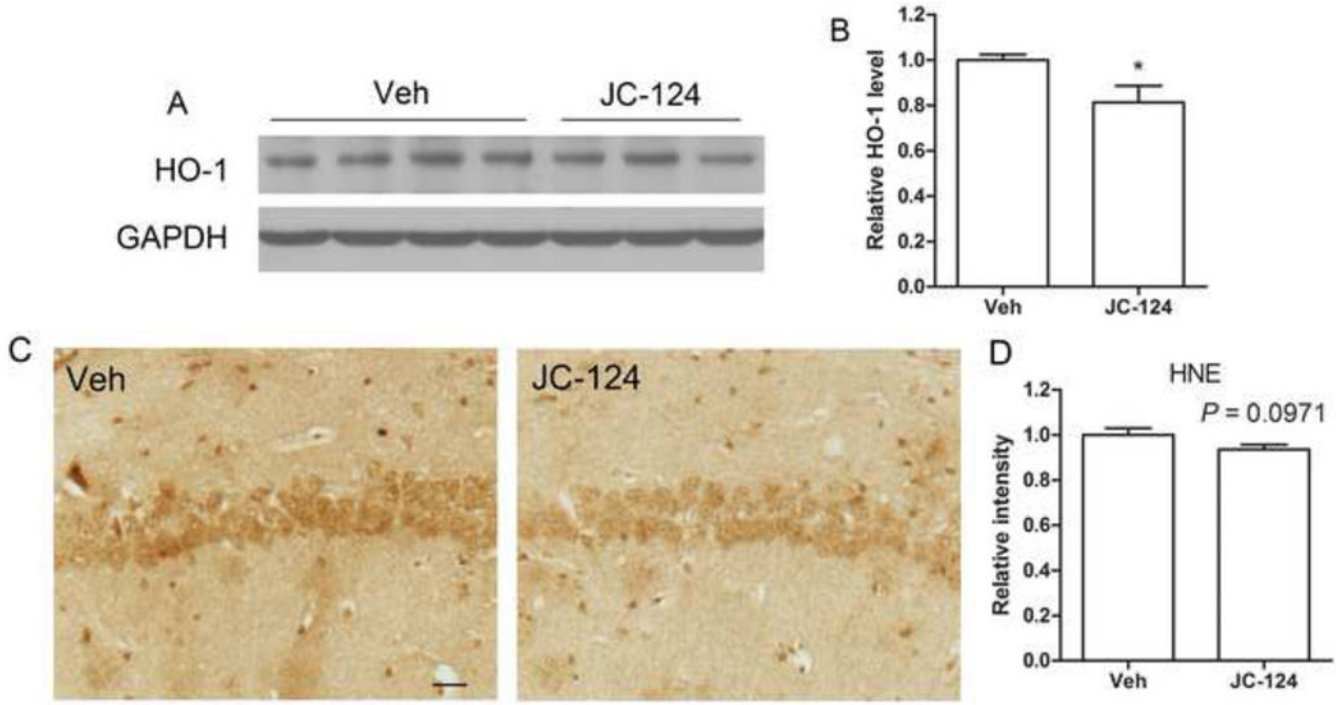

Figure 7. Effect of JC-124 on oxidative stress in TgCRND8 mice

Representative western blot of cortical homogenates (**A**) and quantification analysis (**B**) revealed that the levels of HO-1, an inducible antioxidant enzyme widely used as an oxidative stress marker, were significantly decreased in JC-124-treated CRND8 mice compared to vehicle-treated CRND8 mice. GAPDH was used as an internal loading control. **C**) Representative immunohistochemistry of anti-HNE antibody to detect lipid peroxidation in the hippocampus of JC-124 treated and vehicle-treated CRND8 mice. Scale bar represents 25 μm. (**D**) Relative neuronal intensity of HNE was measured and normalized to the vehicle-treated CRND8 mice. Data represent mean ± SEM, Student's *t*-test, $*P < 0.05$.

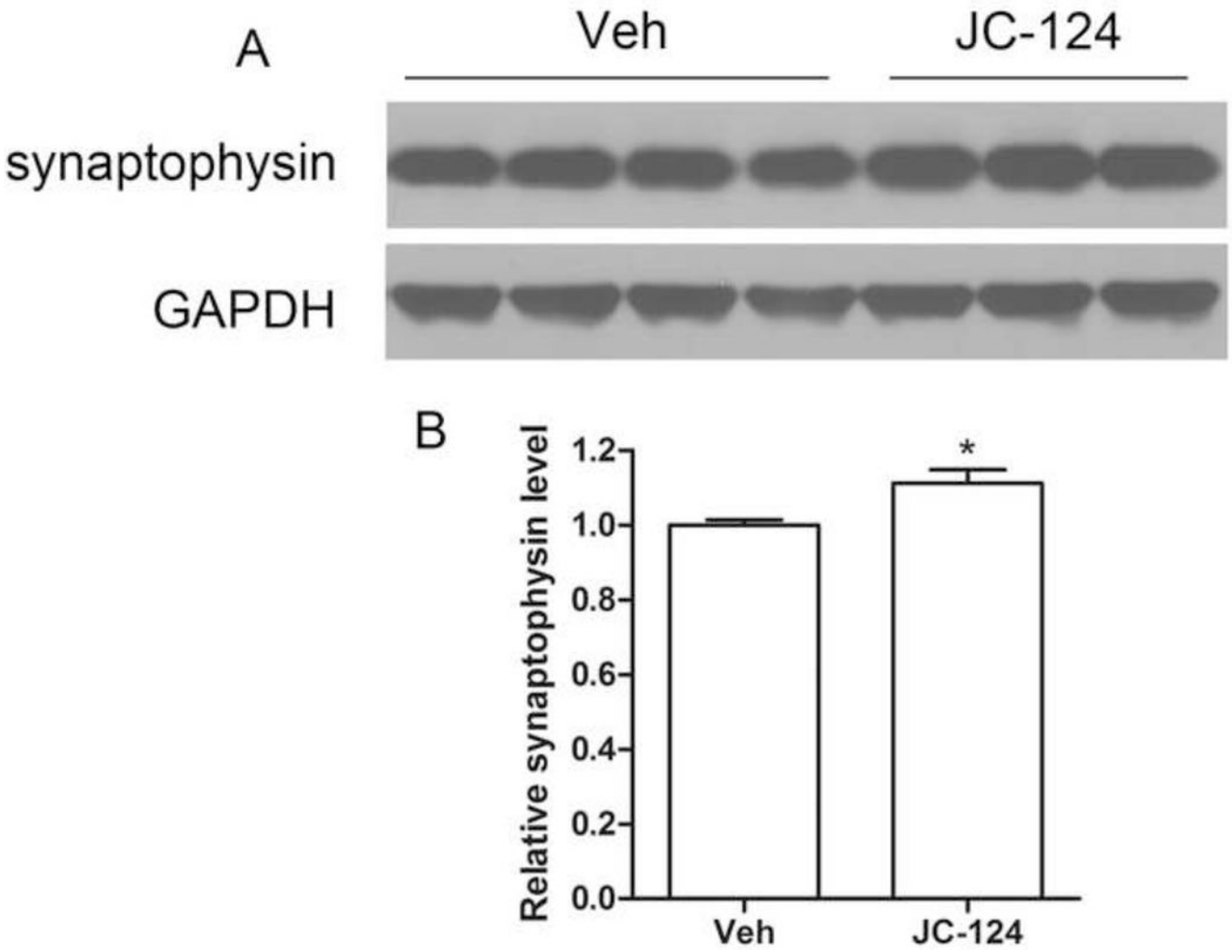

Figure 8. Effect of JC-124 on synaptic marker in TgCRND8 mice

Representative western blot of cortical homogenates (**A**) and quantification analysis (**B**) revealed that the levels of synaptophysin were significantly increased in JC-124-treated CRND8 mice compared to vehicle-treated CRND8 mice. GAPDH was used as an internal loading control. Data represent mean ± SEM, Student's *t*-test, $*P < 0.05$.